

Low-Temperature Polyol Synthesis of Nanocrystalline Cobalt

E. Chávarri-Pajares, *O. Perales-Perez, E. Rodríguez, J. Perez, R. Singhal and M. S. Tomar

University of Puerto Rico at Mayagüez, Mayagüez, PR 00680-9044, *ojuan@uprm.edu

ABSTRACT

The systematic study of the synthesis of nanocrystalline cobalt in trimethylene glycol (TMEG) is presented. The solution chemistry affected the kinetics of the metal-forming reaction and hence, the stability of cobalt phases. The addition of OH⁻ ions into the cobalt solution in TMEG not only accelerated the formation of the magnetic phase but also affected the stability of the metallic precipitate. Depending on the OH/Co mole ratio and the type of cobalt salt, hcp, fcc and metastable pseudo-cubic ϵ -Co phases were formed. Highly monodisperse ϵ -Co nanoparticles were produced when cobalt acetyl-acetonate salt was used instead of the acetate one. Furthermore, the presence of Pt ions in starting solutions results in a dramatic shortening of the reaction time. The saturation magnetization (M_s) and coercivity (H_c) values of the cobalt samples ranged from 80 to 110 emu/g and 101 to 211 Oe, respectively. The higher coercivity of 248 Oe was found when CoPt co-existed in the precipitates produced at 214°C.

Keywords: cobalt, cobalt-platinum, nanocrystals, polyol process, epsilon cobalt, ferromagnetism.

1 INTRODUCTION

The synthesis of magnetic nanoparticles exhibiting high coercivity is of great technological importance because of their use in magnetic recording media, ferrofluids or in the production of permanent magnets. To date, numerous physical and chemical methods have been developed to synthesize metal nanocrystals, including sputtering, metal evaporation, grinding, electro deposition, solution phase metal salt reduction and neutral organometallic precursor decomposition [1, 2]. Among solution-based approaches, the polyol synthesis route can provide strong enough reducing condition to precipitate metallic phases from hydroxides and salts [3]. The process is simple and environmental friendly. Moreover, it also permits the manipulation of the solid formation rate, leading to the production of metastable phases, a tailored phase composition, a tuned particle size and monodispersity at the micro and nanoscale [4-6]. Keeping this in view, the present work is focused on the synthesis of nanocrystalline Co particles in boiling TMEG solutions. The influence of the type of cobalt salt, OH/Co mole ratio, concentration of cobalt and co-existence of Pt ions in starting solutions, on the stability conditions of the cobalt phases was investigated. Structural and magnetic properties were also investigated and reported.

2 EXPERIMENTAL

2.1 Materials

All chemicals were of chemical grade and used without any further purification. TMEG (boiling point 214°C) was used as the solvent and reducing agent. Co(II) acetate tetrahydrate, Co(ac)₂, and Co(II)-acetylacetonate, Co(acac)₂, salts were used as precursors. Sodium hydroxide (NaOH) was used as the source for hydroxyl ions. Hexachloroplatinate salt (H₂PtCl₆) was also added to the reacting solution when seeding-assisted precipitation was evaluated.

2.2 Synthesis of Nanocrystalline Cobalt

TMEG solutions of Co and NaOH were placed in a three-neck flask and heated up to 214±5 °C under a gentle mechanical stirring ('heating stage'). The amount of NaOH was determined according the required OH/Co mole ratios ('R'). The solution was refluxed for different times under polyol boiling conditions. The time required for the formation of a dark gray solid after the reactants reached at selected reaction temperature was defined as the 'reaction time'. The final suspension was quenched in ice and was centrifuged to obtain the powder. The powder was then washed four times with ethanol and finally stored at room temperature. In later experiments, Pt ions were added to the reacting solutions to accelerate the formation of the magnetic solid, by the formation of pre-existent nuclei in solution.

2.3 Products Characterization

The crystal structure of as-synthesized cobalt nanocrystals was studied by x-ray powder diffraction (SIEMENS D500 Cu-K_α radiation). Scanning Electron Microscopy (JEOL JSM-5410 LV) was used to determine the morphology of the precipitates. M-H hysteresis loops were measured at room temperature in a MPMS SQUID unit.

3 RESULTS AND DISCUSSION

3.1 Effect of the OH/Co Mole Ratio and Type of Cobalt Salt

i. XRD Analyses

Figure 1 shows the XRD patterns corresponding to the precipitates obtained after 4 hours of reaction. In absence of

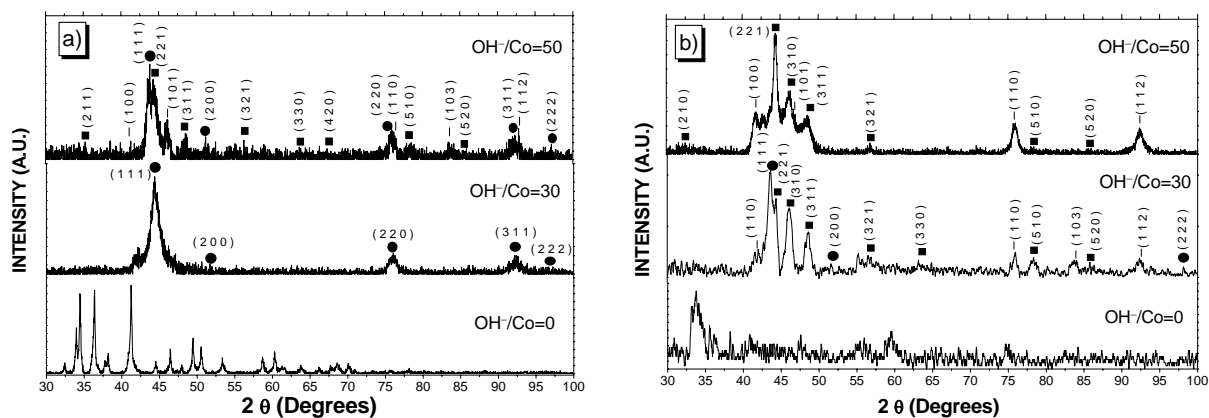


Figure 1: XRD patterns of as-synthesized cobalt powders from 0.01M Co solutions using: a) $\text{Co}(\text{ac})_2$, and b) $\text{Co}(\text{acac})_2$ precursors and 4 hours of reaction time. Peaks corresponding to fcc (●), hcp (◊) and ϵ (■) cobalt phases are indicated.

OH^- ions, i. e. ' R '=0, only hydroxi-alcoxide like intermediate was formed when both Co salts were used. However, the intermediate obtained from $\text{Co}(\text{ac})_2$ seems to be more crystalline than the one precipitated from $\text{Co}(\text{acac})_2$ solutions. Metallic cobalt was formed only for ' R ' values higher than 10. The presence of OH^- ions may have accelerated the dissolution of the intermediates to give dissolved cobalt species, which were finally reduced into the metallic state. This catalytic role of OH^- ions in the formation of metallic cobalt was also reported in our earlier works [3]. Figure 1 also evidenced that the addition of OH^- ions also affected the stability of metallic cobalt phases. fcc-Co was the predominant phase at ' R '=30 when $\text{Co}(\text{ac})_2$ was used. Although in minor proportion, metastable ϵ -Co co-existed with fcc-Co at ' R '=50 (Figure 1-a). As figure 1-b shows, ϵ -Co was the predominant phase that co-existed with hcp- and fcc-Co, when $\text{Co}(\text{acac})_2$ was used instead of $\text{Co}(\text{ac})_2$. Moreover, the relative amount of hcp-Co phase was increased at ' R '=50. The average crystallite size, estimated by using Scherrer's equation, was around 11-15 nm for the fcc- and ϵ -Co phases. The use of $\text{Co}(\text{acac})_2$ could have accelerated the kinetics of the intermediate dissolution-cobalt reduction reactions and hence, the formation of metastable hcp and ϵ nanostructures.

ii. SEM Observations

Figure 2 shows the SEM images of cobalt nanocrystals, obtained at different ' R ' values using $\text{Co}(\text{ac})_2$ as precursor. As evident, the morphological features are quite different depending on the synthesis conditions. The solids produced at ' R '=0 consisted of monosize bi-pyramidal intermediate particles (Figure 2-a). The SEM image of figure 2-b suggests a partial dissolution of the intermediate, attributed to the presence of OH^- ions, when the ' R ' value was 10. Strongly aggregated sub-micron individuals were obtained for ' R '=50. A different morphological pathway was followed when $\text{Co}(\text{acac})_2$ salt was used as precursor. As shown in figure 3, the intermediate produced at ' R '=0 and 10 (Figures 3-a and b, respectively) consisted of sub-micrometric grains. This morphological feature would

suggest an enhanced solubility of the intermediate conducive to the formation of metastable cobalt phases. The monodispersity in Co particles synthesized at ' R '=50 (Figure 3-c) can be due to the adsorption of negative acetylacetonate species, which would prevent excessive aggregation between particles.

iii. Magnetic Characterization

SQUID analyses of cobalt precipitates synthesized at ' R '=50 showed a well-saturated M-H loop with saturation magnetization values, M_s , around 84 emu/g (Figure 4). The coercivity (H_c) of Co nanocrystals were 168 Oe and 211 Oe for the solids produced from $\text{Co}(\text{ac})_2$ and $\text{Co}(\text{acac})_2$, respectively. The corresponding remanence (M_r) varied between 6 and 8 emu/g. The coercivity exhibited by these samples was attributed to the presence of the hcp-Co phase, which was present in a larger proportion when the $\text{Co}(\text{acac})_2$ salt was used. It is well known that metastable ϵ - and fcc-Co phases do not exhibit remarkable ferromagnetism [3].

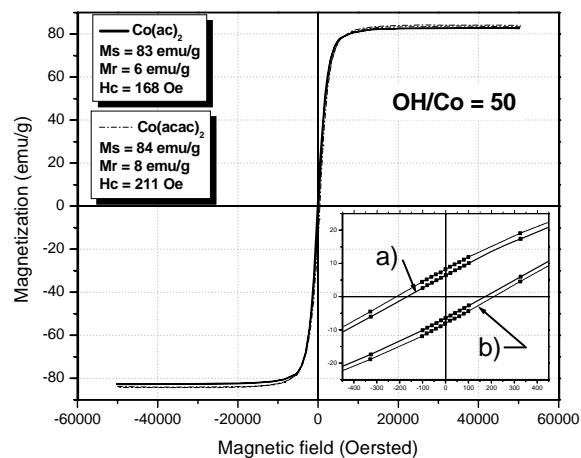


Figure 4: M-H loops for Co powders synthesized from 0.01M $\text{Co}(\text{ac})_2$, 'a', or 0.01M $\text{Co}(\text{acac})_2$, 'b', solutions. The insets show the M-H loop around the origin.

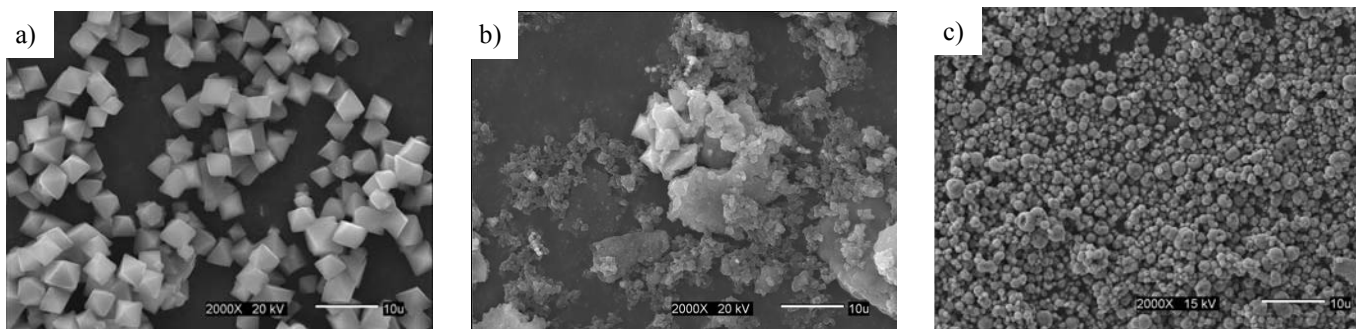


Figure 2: SEM pictures of cobalt particles synthesized in TMEG at different ‘R’ values and using $\text{Co}(\text{ac})_2 \cdot 4\text{H}_2\text{O}$ as source of cobalt ions: a) ‘R’=0; b) ‘R’=10 and c) ‘R’=50. The scale bar represents 10 μm .

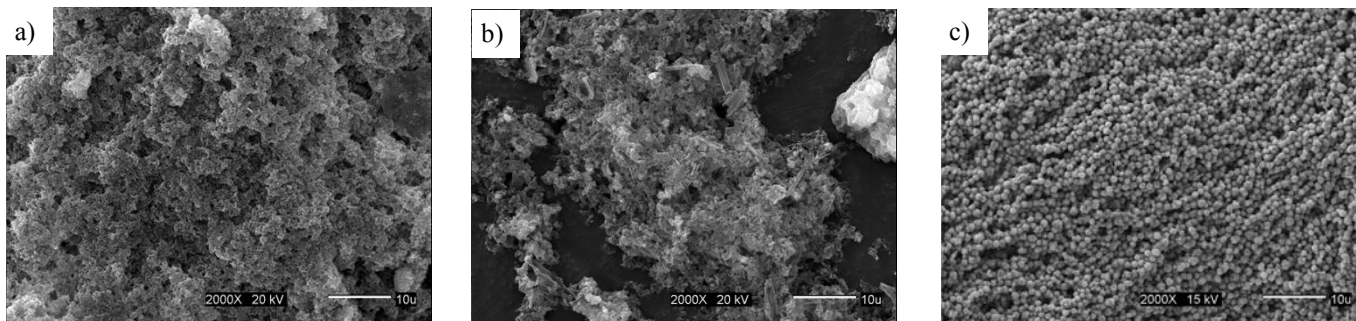


Figure 3: SEM pictures of cobalt particles synthesized in TMEG at different conditions using $\text{Co}(\text{acac})_2$ as source of cobalt ions: a) ‘R’ of 0; b) ‘R’ of 10 and c) ‘R’ of 50. The scale bar represents 10 μm .

3.2 Effect of the Concentration of Co Ions

In order to evaluate the possibility of accelerating the reduction reaction by increasing the ratio of reducing agent to cobalt ions, reduction tests were carried out at different Co concentrations in TMEG.

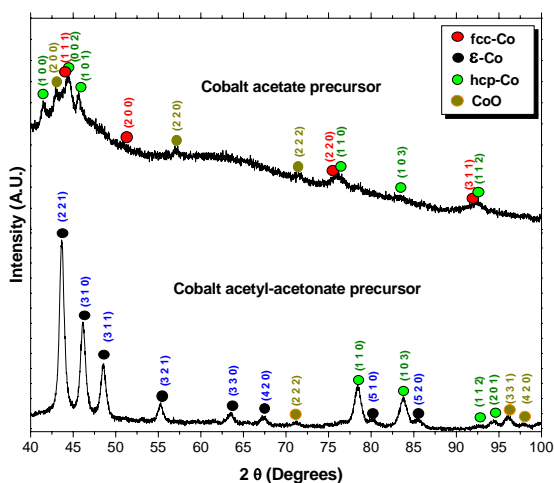


Figure 5: XRD patterns for Co particles synthesized from different precursors. The reaction time was 4 hours and ‘R’ of 50.

The XRD patterns of figure 5, correspond to the solid synthesized at 0.0025M Co after 4 hours of reaction and at ‘R’=50. A mixture of fcc- and hcp-Co, was observed when $\text{Co}(\text{ac})_2$ was used. The presence of CoO was attributed to

the oxidation of the sample during extended XRD measurement times. On the contrary, only metastables ϵ - and hcp-Co phases were precipitated from $\text{Co}(\text{acac})_2$. The well defined and sharp XRD peaks of the ϵ -Co phase suggest its high crystallinity.

3.3 Effect of the Co-existence of Pt Ions in Starting Solutions

i. XRD analyses

Our earlier works suggested the promoting effect of Pt ions on the formation of cobalt precipitates [7-9]. Accordingly, precipitation tests were undertaken by varying the Pt/Co mole ratio in starting solutions between 0.15 and 1.1. The ‘R’ value was 50 in all these experiments. The presence of Pt ions accelerated the cobalt formation dramatically; the magnetic phase was detected after one minute of reaction, instead of the 4 hours required in its absence. The co-existence of ϵ - with hcp-Co (Figure 6), was suggested by XRD analyses of samples produced at ‘R’=50, 10 minutes of reaction and 0.08 moles of Pt in starting solutions. The excess of Pt was present as fcc-Pt. Moreover, the presence of (110), (111) and (112) peaks suggest that ferromagnetic ordered fct-Co phase would have been formed. To our knowledge, this is the first report on the direct formation of fct-CoPt alloy at such a low temperature as 214°C, after an extremely short reaction time and with no need of annealing. Apparently, the reduction of cobalt was so accelerated that part of it could get alloyed with Pt during the solid formation process.

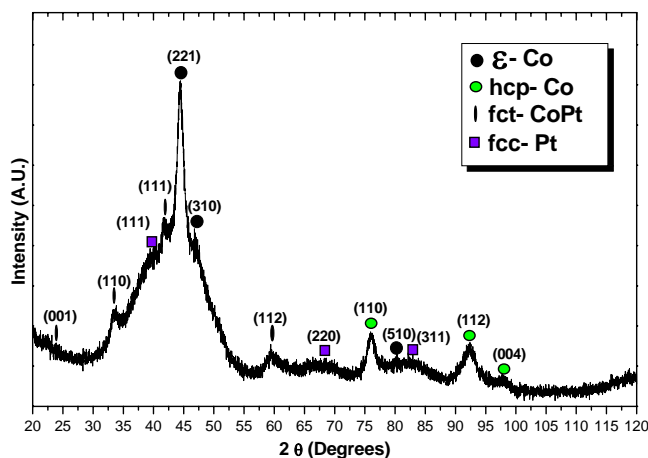


Figure 6: XRD patterns of as-synthesized Co particles at 'R'= 50 and a Pt/Co mole ratio of 0.15. XRD analysis revealed the coexistence of hcp, fcc, ϵ -Co; fcc-Pt and ordered fct-CoPt.

ii. SEM Observations

As Figure 7 shows, metallic precipitates consisted of tiny particles in the sub-micrometric range. The extremely small size of the precipitates is attributed to the enhancement of the nucleation rate by the presence of pre-existent nuclei under kinetically enhanced precipitation conditions.

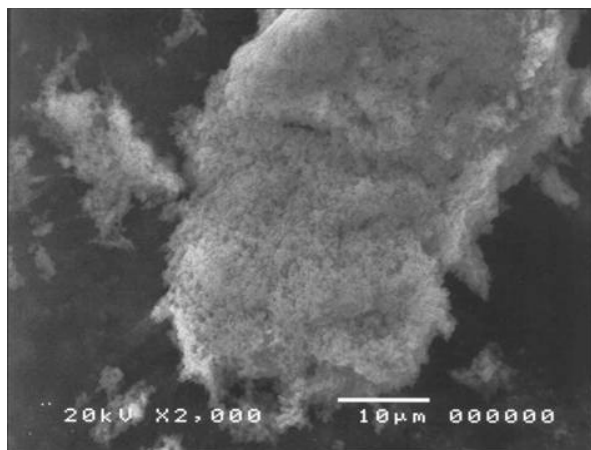


Figure 7: SEM picture of cobalt particles synthesized at 0.0025 M Co(acac)₂ and a Pt/Co mole ratio of 0.15.

iii. Magnetic Characterization

SQUID analyses at RT of cobalt products resulted in saturated M-H loops with M_s of 10 to 70 emu/g and H_c values between 188 and 248 Oe. The variation in M_s values can be due to the different proportion of diamagnetic Pt reduced when various Pt/Co mole ratios were present in starting solutions. The highest M_s and H_c values were obtained at Pt/Co mole ratio of 0.15, 0.0025M Co and 10 minutes of reaction. This coercivity value was attributed to the presence of the hcp-Co phase and the fct-CoPt structure [7-9].

4 CONCLUDING REMARKS

We have successfully synthesized nanocrystalline and highly monodisperse ϵ -Co nanoparticles. The hcp-Co phase was also present, although in minor proportion. The coexistence of Pt ions in starting solutions not only promoted the nucleation rate and accelerated the cobalt reduction but also induced the formation of ordered fct-CoPt nanocrystals at low temperature (214°C). SQUID analyses suggested that nanocrystals exhibited a predominant ferromagnetic behavior at RT. M_s and H_c became as high as 248 Oe when fct-CoPt, in addition to ϵ - and hcp-Co, was formed.

ACKNOWLEDGEMENTS

This material is based upon work supported by the NSF under Grant No. 0351449. Any opinions, findings and conclusions or recommendations expressed in this material are those of the author(s) and do not necessarily reflect the views of the National Science Foundation (NSF). Thanks are also extended to NSF-Start Up Program for providing partial support for this research. We also appreciate the support from E. Calderón with SQUID measurements.

REFERENCES

- [1] G. Schmid, Nanoparticles from Theory to Application, 2004, Ed. Wiley, pp. 204-216.
- [2] Shouheng Sun and C. B. Murray, J. Appl. Phys., 1999, Vol. 85, N^o 8, pp. 4325-4330.
- [3] O. Perales, B. Jeyadevan, N. Chinnasamy, K. Tohji and A. Kasuya, Proc. Int. Symp. on Cluster Assembled Mater, Series 3, pp. 105-108.
- [4] V. Puentes and K. Krishnan, Appl. Phys. Letters, 2001, Vol. 78, N^o 15, pp. 2187-2189.
- [5] D. Larcher and R. Patrice, J. of Solid State Chemistry, 2000, 154, pp. 405-411.
- [6] S. Cha, Ch. Mo, K. Kim and S. Hong, J. Mater Res., 2005, Vol. 20, N^o 8, pp. 2148-2153.
- [7] C. Chinnasamy, B. Jeyadevan, K. Shinoda and K. Tohji, J. Appl. Phys., 2003, Vol. 93, N^o 10, pp. 7583-7585.
- [8] V. tzizios, D. Niarchos, G. Margariti, J. Fidler and D. Petridis, Institute of Physics Publishing, 2005, Vol. 16, pp. 287-291.
- [9] M. Mizuno, Y. Sasaki, M. Inoue, C. Chinnasamy, B. Jeyadevan, D. Hasegawa, T. Ogawa, M. Takahashi, K. Tohji, K. Sato and S. Hisano, J. Appl. Phys., 2005, Vol. 97, pp. 10j301 1-3.